



FULL PAPER

Promising new catalytic properties of a Co (II)-carboxamide complex and its derived Co₃O₄ nanoparticles for the Mizoroki-Heck and the Epoxidation reactions

Mahsa Kiani¹ | Mojtaba Bagherzadeh¹ | Soraia Meghdadi² |
Farzaneh Fadaei-Tirani³ | Maryam Babaie² | Kurt Schenk-Joß⁴

¹Department of Chemistry, Sharif University of Technology, Tehran, 11155-3516, Iran

²Department of Chemistry, Isfahan University of Technology, Isfahan, 84156-83111, Iran

³Institute of Chemical Sciences and Engineering, École Polytechnique Fédérale de Lausanne, Lausanne, CH-1015, Switzerland

⁴Institute of Physics, École Polytechnique Fédérale de Lausanne, Lausanne, CH-1015, Switzerland

Correspondence

M. Bagherzadeh, Department of Chemistry, Sharif University of Technology, Tehran 11155-3516, Iran.
Email: bagherzadeh@sharif.edu

The new Co(II) - carboxamide complex (**1**) and Co₃O₄ nanoparticles (**2**), by way of thermal decomposition of (**1**) have been efficiently synthesised in the environment-friendly. X-ray diffraction reveals a slightly distorted octahedral coordination of cobalt (four nitrogens and two oxygens) in (**1**) and regular octahedral or tetrahedral ones (oxygen only) in (**2**). The investigation of (**1**) and (**2**) in the Mizoroki-Heck and epoxidation of alkenes reactions showed them both to be powerful, green and inexpensive catalysts.

KEYWORDS

co (II)-carboxamide complex, Co₃O₄ nanoparticles, epoxidation, Mizoroki-Heck, X-ray crystal structure

1 | INTRODUCTION

C-C bond-forming reactions are currently attracting the attention of scientists owing to their significant applications in pharmaceutical,^[1] agrochemical^[2] and chemical industries.^[3,4] The Mizoroki-Heck (MH) reaction is considered the most strategic process for the arylation of olefins through a palladium-catalysed C-C bond-forming reaction.^[5-9] Nowadays, vigorous attempts at designing a green, simple, cost-effective and efficient approach for carrying out the MH reaction are being undertaken, but there is still ample room for improvement.^[10-12] In particular, a fully green solvent and the replacement of palladium with a more accessible and cheaper metal might amount to a true breakthrough.^[13-16]

Alkene epoxidations (AE) are ubiquitous in industry; for instance, epoxides are versatile intermediates in the production of food additives, fine chemicals, drug intermediates and even agrochemicals.^[17,18] Current methods

present problems, however, such as high cost, difficulty in recovering catalysts and generation of large quantities of acidic and chlorinated waste. In recent years, nanocatalysts have emerged as robust, heterogeneous alternatives to homogeneous catalysts.^[19]

Thiazole-based compounds are heterocycles found in natural products; they are considered bioactive^[20,21] and useful for catalytic reactions.^[22] Furthermore, it has been proven that designing a thiazole coupled with an amide group could enhance some of the biological activities. Amide bonds are present in numerous industrially important compounds and bioactive natural products containing the primary structure of proteins.

Pyridine-based carboxamide ligands have also been broadly scanned with respect to several biological and catalytic applications, including asymmetric allylic alkylation^[23] and epoxidation.^[24] Finally, the synthesis of carboxamides is being intensely optimised because of its critical role in industrial and pharmaceutical fields.^[25]

Recently, the behaviour of pyridine carboxamides towards transition metals such as cobalt has been widely investigated because of their capacity to form coordination polymers^[26,27] and their electric or catalytic properties.^[28,29] Nanoparticles (np) of cobalt oxide, a p-type semiconductor, have also attracted extensive interest owing to their potential applications in heterogeneous catalysis,^[30] Li-ion rechargeable batteries,^[31,32] magnetic materials^[33,34] and gas sensors^[35] to name a few only.

In this context, we have synthesised and fully characterised the novel carboxamide-based ligand N-(thiazole-2-yl) picolinamide (**Htp**) and its cobalt (II) complex (**1**). Our synthesis of **Htp** has relied on the environment-friendly TBAB in order to replace pyridine and increase the yield of the product.^[30,36,37] From the simple precursor (**1**) we have also produced Co₃O₄ nps (**2**). We then studied the catalytic properties of (**1**) and (**2**)^[38] in the MH cross-coupling^[13,39] and AE^[40] reactions. For investigating the catalytic application, the fully green solvent polyethylene glycol (PEG) was used and the palladium was replaced with the more accessible and inexpensive cobalt. Indeed, the cobalt complex is able, as an efficient, green, cost-effective and optimised heterogeneous catalyst, to process both AE and MN reactions simultaneously.

2 | EXPERIMENTAL

2.1 | Materials and general methods

All solvents and chemicals were of commercial reagent grade and used as received from Aldrich and Merck. Elemental analyses were performed on a Perkin-Elmer 2400II CHNS-O elemental analyser. Fourier transform infrared (FTIR) spectra of the synthesised samples were recorded on a Bruker Tensor 27 spectrometer using KBr pellets for sample preparation at room temperature. UV-vis analyses were performed on a CARY 100 Bio VARIAN spectrophotometer using quartz cells having a path length of 1.0 cm. The ¹H-NMR spectrum of **Htp** was obtained on a Bruker FT-NMR 500 MHz spectrometer; proton chemical shifts are reported in parts per million (ppm) relative to an internal standard of Me₄Si. Cyclic voltammograms (CV) were recorded on a SAMA 500 Research Analyzer using a three-electrode system: a glassy carbon working-electrode (Metrohm 6.1204.110 with 2.0 ± 0.1 mm diameter), a platinum disk auxiliary electrode and Ag wire as reference-electrode. The glassy carbon-working electrode was manually cleaned with 1 μm alumina polish prior to each scan. CV measurements were performed in DMF with tetrabutylammonium hexafluorophosphate (TBAH) as

supporting electrolyte. The solutions were deoxygenated by purging them with Ar for 5 min. All electrochemical potentials were calibrated versus the internal Fc⁺⁰ (E⁰ = 0.45 V vs. SCE) couple under the same conditions. Thermogravimetric-differential thermal analysis (TG-DTA) was conducted on a NETZSCH STA 449F3 thermal analyser at a constant heating rate of 10 °C min⁻¹ in air. Powder patterns were recorded in the 2θ range of 10°–100° on an MPD-PRO powder diffractometer from PANalytical using Ni-filtered CuKα radiation. The morphology and composition of the Co₃O₄ n.p.s were observed by a field emission scanning electron microscopy (FE-SEM, MIRA3 TESCAN). Gas chromatographic (GC) analyses were performed on an Agilent Technologies 6,890 N, equipped with a 19,019 J-413 HP-5, 5% phenyl methyl siloxane, and a capillary column (60.0 m × 250 μm × 1.00 μm).

2.2 | Synthesis

2.2.1 | Synthesis of N-(thiazole-2-yl) picolinamide (**Htp**)

A mixture of 3.22 g (10 mmol) of triphenylphosphite, 1.61 g (5 mmol) of TBAB, 1.23 g (10 mmol) of picolinic acid and 1 g (10 mmol) of 2-aminothiazole in a 25 ml round-bottomed flask was placed in an oil bath. The reaction mixture was heated until a homogeneous solution was formed which was kept stirring for 1 hr at 120 °C; then the viscous solution was cooled to room temperature and treated with 5 ml of cold methanol. The resulting light yellow solid was filtered-off and washed with cold methanol. Yield 79%. Anal. Calc. for C₉H₇N₃OS (205.32 g mol⁻¹): C, 52.67; H, 3.44; N, 20.47; S, 15.61. Found: C, 52.31; H, 3.46; N, 20.34; S, 15.21%. FT-IR (KBr, cm⁻¹) ν_{max}: 3175 (NH), 1,675 (C=O_{amide}), 1,525 (C-N); UV-visible (acetonitrile): λ_{max} (nm) (ε, L mol⁻¹ cm⁻¹): 287 (32,800), 221 (32,440). ¹H NMR (CDCl₃, 500 MHz): 7.36 (d, H_c), 7.58 (d, H_b), 7.73 (m, H_e), 8.12 (m, H_f), 8.19 (d, H_d), 8.77 (d, H_g), 11.94 (s, NH).

2.2.2 | Synthesis of [Co (tp)₂(H₂O)₂].C₂H₅OH (**1**)

Co (CH₃COO)₂·4H₂O (25 mg, 0.1 mmol) was added to a solution of **Htp** (41 mg, 0.1 mmol) in dichloromethane (35 ml); this mixture was stirred for 4 hr. Then it was filtered and 20 ml of ethanol were added to the leach solution. Bright orange crystals of bis (N-(thiazole-2-yl) picolinamide) di aqua cobalt (II) ethanol solvate, suitable for X-ray diffraction, were obtained by slow evaporation

of a solution in ethanol-dichloromethane at refrigerator temperature. The crystals were isolated by filtration, washed with cold ethanol and dried in vacuo. Yield 82%. Anal. Calc. for $C_{20}H_{22}CoN_6O_5S_2$ ($549.488 \text{ g mol}^{-1}$): C, 43.72; H, 4.04; N, 15.29; S, 11.67. Found: C, 43.74; H, 3.94; N, 15.21; S, 11.84%. FT-IR (KBr, cm^{-1}) ν_{max} : 1582 ($\text{C}=\text{O}_{\text{amide}}$), 1,552 (C-N) cm^{-1} . UV-visible (acetonitrile): λ_{max} (nm) (ϵ , $\text{L mol}^{-1} \text{ cm}^{-1}$): 522(500), 331 (19,200), 269 (26,400).

2.2.3 | Preparation of Co_3O_4 nanoparticles (2)

In order to prepare n.p.s of Co_3O_4 , the complex **1** was loaded into a crucible which was then heated at a rate of $10 \text{ }^\circ\text{C}/\text{min}$ in an oven in air. After n.p.s of Co_3O_4 had grown at $600 \text{ }^\circ\text{C}$ after 2 hr, the sample was cooled to room temperature and the black Co_3O_4 nanocrystals collected and characterised by FT-IR, FE-SEM and XRD analysis.

2.2.4 | General procedure for the Mizoroki-Heck reaction

All MH reactions were carried out in air. In a round-bottom flask, equipped with a mechanical stirrer and a condenser for refluxing, 0.4 mol% of the catalysts **1** or **2** were added to a mixture of K_3PO_4 (4 mmol), olefin (1.2 mmol) and aryl halide (1 mmol) in 3 ml of solvent. This mixture was heated to $130 \text{ }^\circ\text{C}$ in an oil bath. The progress of the reaction was monitored by GC at the end of the catalysis; then the reaction mixtures were allowed to cool to room temperature and extracted thrice with water and diethyl ether ($3 \times 15 \text{ ml}$). The organic layer was separated from the aqueous one, dried over anhydrous MgSO_4 and evaporated to dryness under reduced pressure to afford the desired product. The residue was purified by column chromatography. The products were characterised by comparing their ^1H NMR spectra with those found in the literature.

2.2.5 | General procedure for the epoxidation reaction

The AE reaction over the **1** or **2** nanocatalysts was carried out at atmospheric pressure by dispersing 0.4 mol % of catalyst into a solution of 0.2 mmol of substrate and 0.4 mmol of t-butyl hydroperoxide [TBHP] in water in $\text{C}_2\text{H}_4\text{Cl}_2$ (1 ml) in a magnetically stirred glass reactor under reflux (at $85 \text{ }^\circ\text{C}$) for a period of 5 hr for **1** and 1 hr

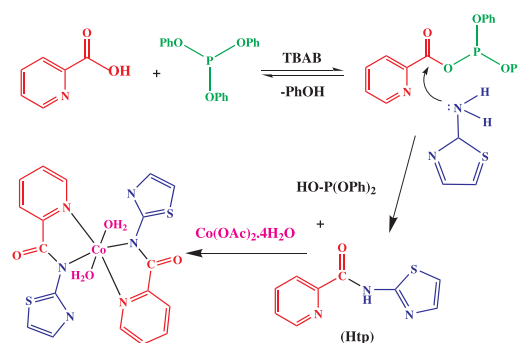
for **2**. The progress of the reaction was monitored by GC at appropriate time intervals and the products were compared with standard samples; the conversion percentage was calculated using the areas of substrate.

2.2.6 | X-ray crystallography

Lath-shaped, orange single crystals of $[\text{Co}(\text{tp})_2(\text{H}_2\text{O})_2]$ were obtained by slow evaporation of an ethanol-dichloromethane solution in a refrigerator. A suitable crystal of $0.56 \times 0.23 \times 0.06 \text{ mm}^3$ was selected, glued to a glass fibre and mounted on a STOE IPDS 2 diffractometer. The crystal was kept at a steady $T = 292(1) \text{ K}$ during the data collection. Data reduction, scaling and absorption corrections were performed using X-Area, 1.36.^[41] The final completeness is 100.00% out to 29.329° in θ . An absorption correction by Gaussian integration was performed using Stoe XRed32 1.31.^[42] The absorption coefficient μ of this material is 0.919 mm^{-1} at a wavelength of ($\lambda = 0.711 \text{ \AA}$) and the minimum and maximum transmission factors are 0.779 and 0.963.

The structure was solved and the space group *Pbcn* (#60) determined by the ShelXT-2014/7^[43] structure solution program using the dual solution method and refined by full matrix least squares on $|F|^2$ using version 2018/3 of *ShelXL*.^[44] All non-hydrogen atoms were refined anisotropically. Hydrogen atoms were placed at calculated positions by means of the "riding" model in which each H-atom was assigned a fixed isotropic displacement parameter with a value equal to $1.2U_{\text{eq}}$ of its parent C-atom ($1.5U_{\text{eq}}$ for the methyl groups), but the hydrogen atoms of the coordinated water molecule were found in a difference map and refined freely.

A residual electron density corresponding to 104.0 electrons was found in a volume of 472.0 \AA^3 in one void. This is consistent with the presence of one molecule of ethanol solvent per formula unit, which accounts for 104.0 electrons. This additional electron density, too



SCHEME 1 Mechanism of the synthesis of Htp and **1** by using the ionic liquid TBAB

disordered to be modelled, was taken into account by using the SQUEEZE/PLATON procedure^[45] (also remember the drying *in vacuo* which might have removed some of the ethanol!). The value of Z' is 0.5. This means that only half of the formula unit is present in the asymmetric unit, with the other half consisting of symmetry equivalent atoms. The crystallographic and refinement data are summarised in Table S1.

3 | RESULTS AND DISCUSSION

3.1 | Synthesis of the ligand Htp and the complex 1

Carboxamide derivatives are usually prepared by reacting amines with the appropriate carboxylic acid in pyridine, in the presence of an activator such as triphenyl phosphate.^[46] Pyridine is, however, being abandoned more and more because of its low efficiency and well-known toxicity; thus, because of their desirable properties, ionic liquids are gradually imposing themselves as an alternative to classic solvents.^[47,48]

The novel bidentate carboxamide ligand **Htp** has therefore been synthesised in the ionic liquid TBAB, with the goal of decreasing the reaction-time, increasing the efficiency and reducing the risks of toxic solvents such as pyridine. Indeed, compared to the classical reaction, the reaction-time was reduced from 4 to 1 hr and the yield increased. The mechanism is assumed to be that shown in Scheme 1.^[49]

The complex (**1**) was prepared by reacting equimolar quantities of **Htp** and cobalt acetate in an ethanol-dichloromethane solution and stirring the latter for 4 hr (Scheme 1). Orange crystals of (**1**), suitable for X-ray diffraction, grew during the slow evaporation of the solvent at refrigerator temperature. Diffraction showed that (**1**) was actually an ethanolate.

3.2 | The crystal structure of 1

The complex **1** is shown in Figure 1 and geometrical details may be found in Table 1. The cobalt (II) centre is 6-coordinated by two pyridine nitrogens [2.131(2) Å], two amide nitrogens [2.167(2) Å] and two water oxygens [2.083(2) Å]. The trans-angles around cobalt (II) lie in the range of 170.12(8)–171.50(10)° and the cis ones in 76.88(8)–97.06(8)°. The metal centre therefore lies in a distorted octahedron. The Co-N (amide) bond is longer than the Co-N (pyridine) one, owing to the equatorial position of the amidic N atoms and the Jahn-Teller effect which leads to the bonds being stretched along this axis.^[50] Hydrogen bonds in **1** are shown in Table S2.

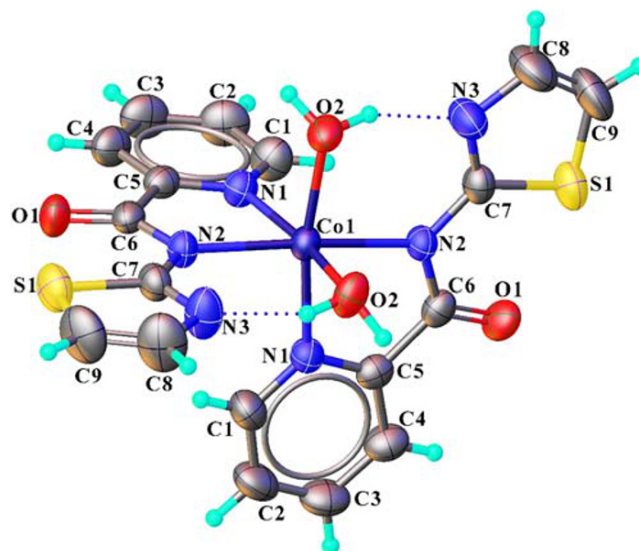


FIGURE 1 Structure of (**1**) with its atomic labelling scheme shown with 50% probability ellipsoids drawn with the help of Olex2. The disordered molecule has been omitted for clarity

TABLE 1 Selected bond Lengths (Å) and angles (°) in [Co(L)₂(H₂O)₂]

Atom	Atom	Length/Å	
Co1	O2 ^[1]	2.0828(18)	
Co1	O2	2.0828(18)	
Co1	N1 ^[1]	2.131(2)	
Co1	N1	2.131(2)	
Co1	N2 ^[1]	2.1667(18)	
Co1	N2	2.1667(18)	
Atom	Atom	Atom	Angle/°
O2 ^[1]	Co1	O2	85.99(12)
O2	Co1	N1 ^[1]	170.13(8)
O2	Co1	N1	92.35(8)
O2 ^[1]	Co1	N1 ^[1]	92.35(8)
O2 ^[1]	Co1	N1	170.12(8)
O2	Co1	N2 ^[1]	93.46(7)
O2	Co1	N2	92.76(7)
O2 ^[1]	Co1	N2	93.46(7)
O2 ^[1]	Co1	N2 ^[1]	92.76(7)
N1 ^[1]	Co1	N1	90.91(11)
N1	Co1	N2 ^[1]	97.06(8)
N1 ^[1]	Co1	N2 ^[1]	76.88(8)
N1 ^[1]	Co1	N2	97.06(8)
N1	Co1	N2	76.88(8)
N2 ^[1]	Co1	N2	171.50(10)

¹1-x, +y, 3/2-z.

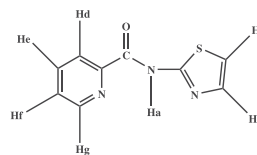
3.3 | Spectroscopic properties

The FTIR spectrum of **Htp** is shown in Figure S1 of the Supporting Information (SI). The amidic $\nu_{\text{N-H}}$ appears at 3175 cm^{-1} , but is absent in the IR spectra of **1**, corroborating the ligand to be coordinated in its deprotonated form.^[51] The sharp $\nu_{\text{C=O}}$ at 1676 cm^{-1} in **Htp** is red-shifted to $1,582\text{ cm}^{-1}$ in **1**, again indicating a deprotonated ligand in **1**. The significant blue-shift of $\nu_{\text{C=O}}$ of medium intensity for the coordinated ($1,552\text{ cm}^{-1}$) relative to the free ligand ($1,529\text{ cm}^{-1}$) gives additional support to the coordination of its amide in their deprotonated form. This is presumably due to the resonance enhancement in the deprotonated amide which in turn leads to the strengthening of the C–N bond,^[49] shown in Figure 2.

The ^1H NMR spectra of **Htp** were measured in CDCl_3 , and reported in Figure S3 of the SI. The structure of **Htp** is shown in Scheme 2. A well-separated peak for the amidic proton N–H is observed around 11.94 ppm.^[21,52] The two doublet peaks appearing at 7.36 ppm and 7.58 ppm, respectively, can be attributed to the H_c and H_b hydrogens of the thiazole ring.^[53] The aromatic protons of the pyridine rings have been observed in the range of 8.77–7.73 ppm.^[21]

The UV–vis data of **Htp** and **1** in acetonitrile are reported in Figures S4 and S5 of the SI. The electronic absorption spectrum of **Htp** includes two bands centred at 221 and 287 nm, assigned to intra-ligand transitions ($\pi \rightarrow \pi^*$ of aromatic rings and $n \rightarrow \pi^*$ of electron pairs of the N atom of carboxamide). **1** shows bands at 269 and 331 nm which are assigned to intra-ligand and charge transfer transitions ($\pi \rightarrow \pi^*$ and $n \rightarrow \pi^*$).^[1]

The thermal behaviour of the precursor **1** has been studied by thermal analysis at a constant heating rate of $10\text{ }^\circ\text{C min}^{-1}$ in the temperature range of $0\text{ }^\circ\text{C}$ to $800\text{ }^\circ\text{C}$. The TG, DTG and DSC curves in Figure 3 show that the decomposition of the complex takes place in two stages.



SCHEME 2 Structure of ligand **Htp**

In the first stage, an endothermic peak at about $110\text{ }^\circ\text{C}$ indicates a weight-loss of roughly 13.75%, which is consistent with the theoretical value of 14.93% for the loss of two water molecules and one molecule of $\text{C}_2\text{H}_5\text{OH}$. In the second stage, the residue gives a sharp exothermic peak at about $320\text{ }^\circ\text{C}$ with an extensive weight loss (86.25%) related to the decomposition of the complex.^[54,55]

Figure 4 presents the XRD pattern of the decomposition product of **1** at $600\text{ }^\circ\text{C}$ for 2 hr. The diffraction pattern contains narrow, but very weak lines corresponding to cubic Co_3O_4 (JCPDS Card No.073–1701) and a huge broad peak probably due to amorphous components and even one or two extraneous lines. The powder pattern is compatible with the Co_3O_4 phase at $600\text{ }^\circ\text{C}$, in fair agreement with the thermal analysis and FT-IR results.

The size and morphology of the cobalt oxide n.p.s have been examined by scanning electron microscopy (FE-SEM) (Figure 5); it can be seen that the n.p.s are spheroids and that their average particle size is 32 nm. The narrow size distribution of the particles shows a uniform size and a homogeneous sphere-like morphology.

3.4 | Electrochemical studies

The electrochemical behaviour of **Htp** and **1** has been studied by cyclic voltammetry in DMF and acetonitrile solutions at a scan rate of 100 mVs^{-1} , with 0.1 M TBAH as the supporting electrolyte and a glassy carbon working-electrode. As expected and previously reported,

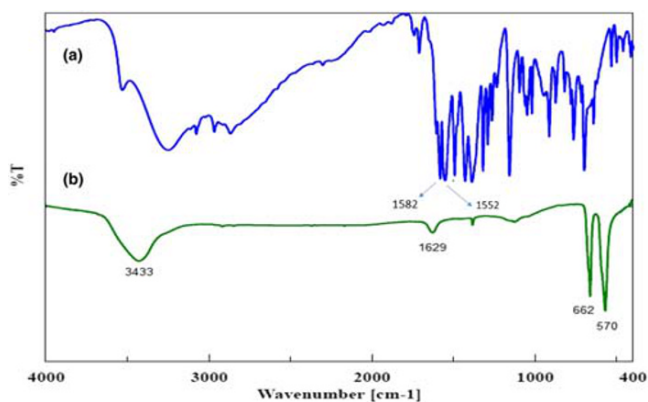


FIGURE 2 FTIR spectrum of (a) **1** (b) **2** nanoparticles

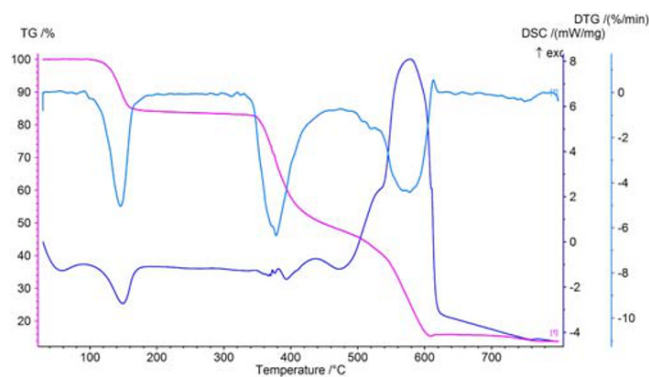


FIGURE 3 TG, DSG and DSC curves of the precursor **1**

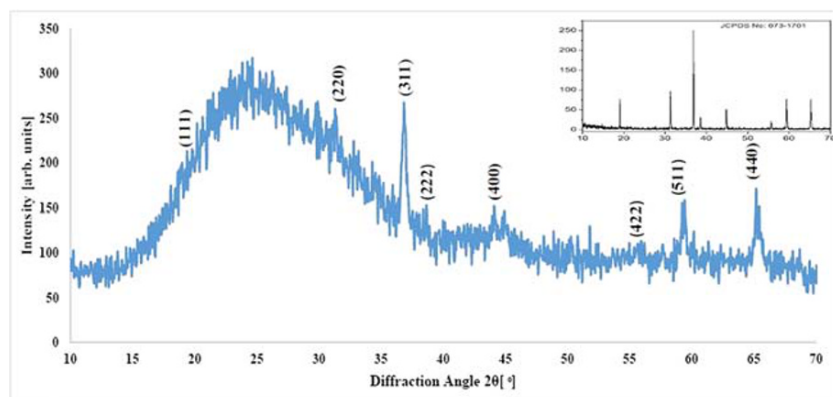


FIGURE 4 XRD pattern of Co_3O_4 showing peak indices and 2θ positions

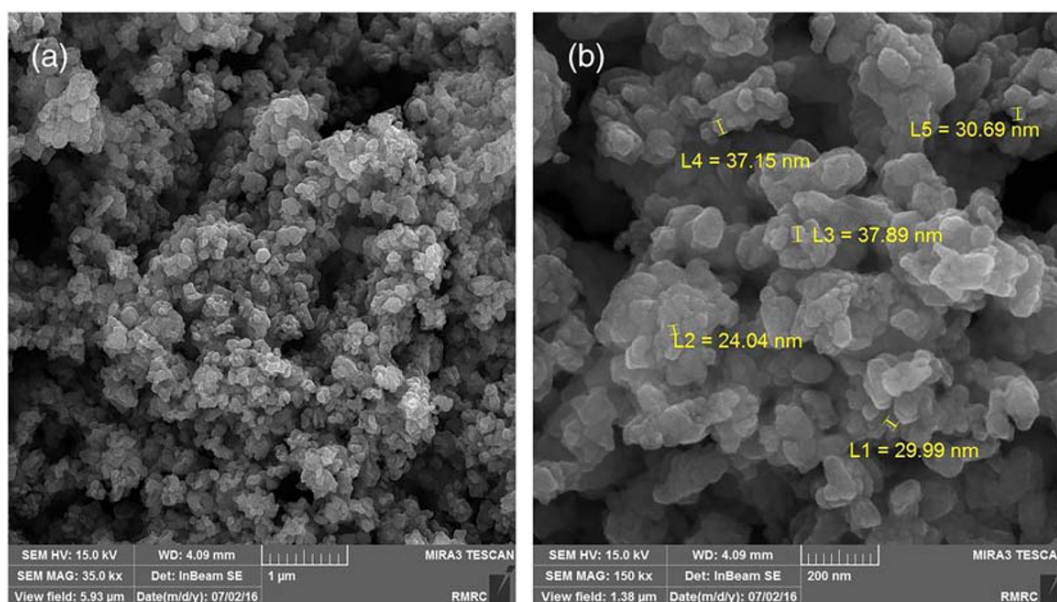


FIGURE 5 FESEM images of the n.p.s (2) (a, 1 μm and b, 200 nm)

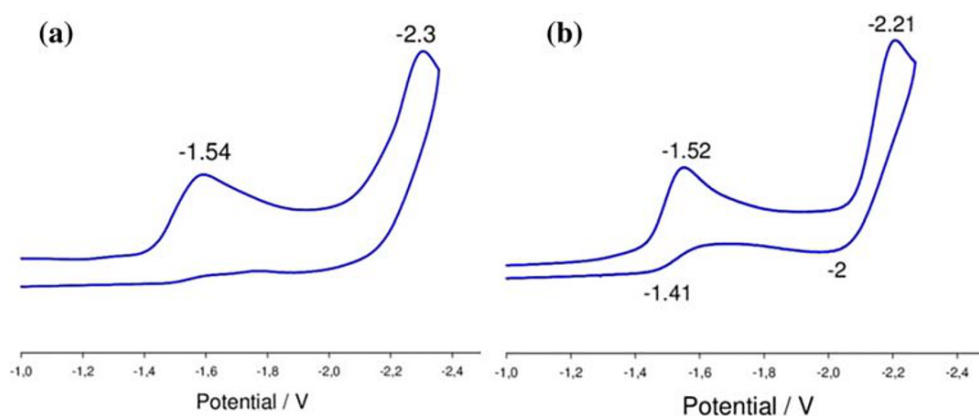


FIGURE 6 Cyclic voltammogram of Htp in DMF (a) and acetonitrile (b) at 298 K, $c \approx 6 \times 10^{-3}$, scan rate = 100 mV s $^{-1}$

the carboxamide ligands are electro-active in common organic solvents^[56]. As shown in the voltammogram of **Htp** in DMF and acetonitrile (Figure 6a and 6b), the two irreversible reduction waves of the thiazole and pyridine rings have been observed at -2.3 and -1.54 V in DMF, and at -2.21 and -1.52 in acetonitrile; they are both shifted to more positive values for **1**.

The electrochemistry of **1** in DMF and acetonitrile (Figure 7a and 7b) shows an irreversible reduction process at $E_{1/2} = -1.51$ and -1.42 V, respectively, which is attributed to the reduction of the $\text{Co}^{\text{II/I}}$ centre. This value is in agreement with those reported in related Co (II) complexes.^[57] These results suggest a one-step redox-reaction with an irreversible mechanism. The last two

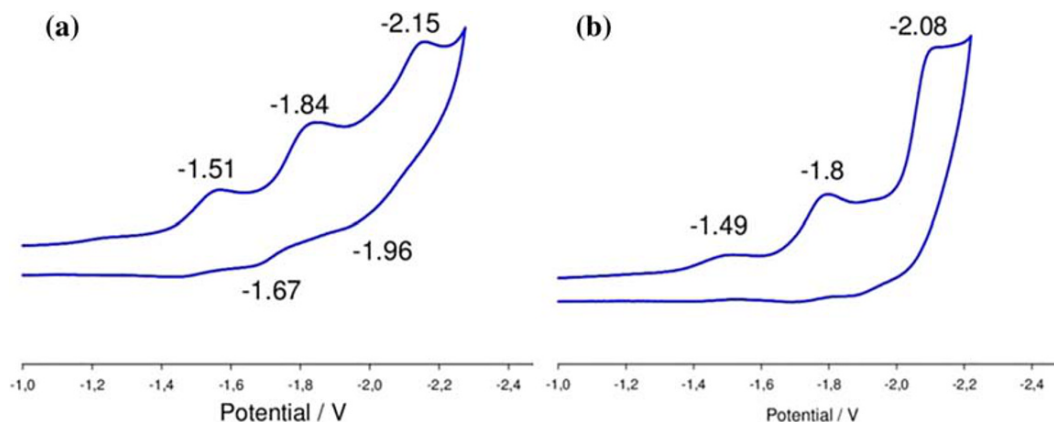


FIGURE 7 Cyclic voltammogram of (1) in DMF (a) and acetonitrile (b) at 298 K, $c \approx 6 \times 10^{-3}$, scan rate = 100 mV s⁻¹

irreversible reduction processes observed at -2.15 and -1.84 V in DMF, and at -2.08 and -1.8 V in acetonitrile are suggested to be mainly ligand-centred, owing to the reduction of the thiazole and pyridine rings, and are shifted to more positive potentials in the Co (II) complex relative to **Htp**.^[58]

3.5 | Catalytic effects

The catalytic activity of our catalysts (1) and (2) was first investigated in the model MH coupling reaction between iodobenzene and methyl acrylate in order to determine the optimal reaction conditions, such as the amount of

TABLE 2 Optimisation of the reaction conditions for the MH reaction of iodobenzene with methyl acrylate in the presence of catalysts (1) or (2)^a

Entry	catalyst	Base	Solvent	Temp(°C)	Time(hr)	Yield (%) ^b
1	1	K ₂ CO ₃	DMSO	130	24	75
2	1	K ₂ CO ₃	DMA	130	24	25
3	1	K ₂ CO ₃	DMSO+H ₂ O	130	24	64
4	1	K ₂ CO ₃	DMA + H ₂ O	130	24	15
5	1	K ₂ CO ₃	PEG	130	24	77
6	1	K ₂ CO ₃	DMF	130	24	15
7	1	TEA	DMSO	130	24	97
8	1	TEA	PEG	130	24	98
9	1	KOH	PEG	130	24	50
10	1	K ₃ PO ₄	PEG	130	24	10
11	1	Na ₃ PO ₄	PEG	130	24	>99
12	1	K ₃ PO ₄	DMSO	130	24	65
13	1	K ₃ PO ₄	PEG	130	12	77
14	1	K ₃ PO ₄	PEG	130	6	>99
15	1	K₃PO₄	PEG	130	2	>99
16	1,2	K ₃ PO ₄	PEG	r.t	24	—
17	1	K ₃ PO ₄	PEG	80	6	>99
18	1	K ₃ PO ₄	PEG	80	2	64
19	2	K ₃ PO ₄	PEG	130	24	>99
20	2	K ₃ PO ₄	DMSO	130	24	88
21	2	K₃PO₄	PEG	130	2	95

^aThe reaction was carried out with iodobenzene (1.0 mmol), methyl acrylate (1.2 mmol), base (4 mmol), Catalyst (0.4 mol %), solvent (3.0 ml).

^bGC yield.

catalysts, solvents, bases, temperature and time of reaction in the presence of a catalyst (Table 2). Firstly, different solvent such as DMSO, DMA, a mixture of DMSO + H₂O (2:1), a mixture of DMA + H₂O (2:1), PEG and DMF were examined, of which PEG and DMSO afforded the maximal yield of methyl cinnamate. Secondly, the same reaction was carried out in different bases, such as, K₂CO₃, TEA, KOH, K₃PO₄, and Na₃PO₄ of which K₃PO₄

was found to be most effective in PEG. Thirdly, the effect of the amount of catalysts was also examined and the best result was obtained by using 0.4 mol % of the catalyst. Finally, the reaction was examined without any catalyst and was found to be very inefficient (Table 2, entry 22). Therefore, the optimal reaction conditions in this catalytic reaction are: iodobenzene (1 mmol), methyl acrylate (1.2 mmol), K₃PO₄ (4 mmol) and catalysts

TABLE 3 Scope of the MH cross coupling reaction for (1) or (2)^a

Entry	X	R	Olefin	Yield(%) ^b	
				[Co (tp) ₂ (H ₂ O)].C ₂ H ₅ OH (1)	Co ₃ O ₄ (2)
1	I	H	Methyl acrylate	99	95
2	I	H	Butyl acrylate	98	77
3	I	H	Ethyl acrylate	>99	75
4	I	H	Styrene	>99	61
5	I	H	α-methyl styrene	95	69
6	I	H	4-methyl styrene	94	65
7	I	H	4-methoxy styrene	95	59
8	Cl	H	Methyl acrylate	10	Trace
9	Cl	H	Butyl acrylate	20	15
10	Cl	H	Ethyl acrylate	15	10
11	Cl	H	Styrene	69	45
12	Cl	H	α-methyl styrene	71	52
13	Cl	H	4-methyl styrene	64	48
14	Cl	H	4-methoxy styrene	68	51
15	Br	H	Methyl acrylate	22	11
16	Br	H	Butyl acrylate	25	29
17	Br	H	Ethyl acrylate	29	23
18	Br	H	Styrene	75	55
19	Br	H	α-methyl styrene	78	62
20	Br	H	4-methyl styrene	67	58
21	Br	H	4-methoxy styrene	58	56
22	I	4-NO ₂	Methyl acrylate	98	96
23	I	4-NO ₂	Butyl acrylate	>99	85
24	I	4-NO ₂	Ethyl acrylate	>99	79
25	I	4-NO ₂	Styrene	96	68
26	I	4-NO ₂	α-methyl styrene	96	60
27	I	4-NO ₂	4-methyl styrene	98	58
28	I	4-NO ₂	4-methoxy styrene	97	61

^aThe reaction was carried out with aryl halide (1.0 mmol), alkene (1.2 mmol), K₃PO₄(4.0 mmol) in 3.0 ml PEG. Catalyst (0.4 mol %) at 130 °C for 2 hr.

^bIsolated yield of the pure product after flash chromatography.

(0.4 mol %) in PEG (3 mL) at 130 °C (Table 2, entry 15 for (1) and entry 21 for (2)).

Applying these optimal reaction conditions, the scope of MH coupling reactions of iodobenzene, 4-nitro iodobenzene, chlorobenzene and bromobenzene with various olefins was then examined (Table 3). The coupling of iodobenzene afforded the desired product in quantitative yield (Table 3, entries 1–7). Initially, the electronic nature of the substituent on the olefin was investigated: various olefins containing electron-donating groups such as methoxy or methyl groups provided the respective products in excellent yields and under mild conditions. Aryl halides substituted with a nitro group at the *para* position were more reactive in the coupling reaction than those without substitution (Table 3, entries 22–28). Aryl chlorides are suitable substrates for the MH coupling reaction, because they are extensively available compared to their bromides and iodide analogs. Note that, despite the strong C–Cl bond, we observed a significant conversion in this coupling reaction. While most reported methods require high loadings of a palladium catalyst and difficult conditions,^[59,60] our cobalt complex (1) and nanocrystals (2) activate even aryl chlorides and aryl bromides in the coupling reactions. It is further

noteworthy that aryl chlorides proceeded smoothly with the same amount of cobalt catalyst as used for aryl iodides and aryl bromides, while most of the cobalt reported in MH reactions was totally inactive for aryl chlorides.^[61,62] We report good result in the MH coupling reactions, even for aryl chlorides in the presence of cobalt catalysts. It is important that, shown by NMR spectra, the trans-product has been obtained with 100% selectivity in all MH olefination reactions. It is also important that this activity of cobalt is reported for the first time for the MH reaction.

Encouraged by the promising results in the MH cross-coupling reaction, we turned our attention to the potential of our (1) and (2) in the AE reaction. In order to determine the optimal experimental conditions, the epoxidation of cis-cyclooctene in the presence of (1) was chosen as a model reaction. The effect of the amount of catalyst, the type and amount of oxidants, the solvent and the temperature are summarised in Table 4, which shows that the best result was obtained with cis-cyclooctene (0.2 mmol), TBHP (0.4 mmol) and 0.4 mol % catalyst in DCE (1 ml) at 85 °C for 5 hr (Table 4, entry 9).

In order to assess the applicability of our catalysts, nine different alkenes were used to examine the

TABLE 4 Optimisation of the reaction conditions of the AE reaction of cis-cyclooctene with TBHP in water in the presence of (1)^a

Entry	Catalyst (mol%)	Oxidant (mmol)	Solvent	Temperature	Conversion (%) ^b	Selectivity (%) ^c
1	0.2	H ₂ O ₂ (0.2)	DCE	85	—	100
2	0.2	UHP(0.2)	DCE	85	Trace	100
3	0.2	TBHP(0.2)	DCE	85	60	100
4	0.2	TBHP(0.6)	DCE	85	88	100
5	0.4	TBHP(0.6)	DCE	85	93	100
6	0.6	TBHP(0.6)	DCE	85	94	100
7	0.7	TBHP(0.6)	DCE	85	94	100
8	0.8	TBHP(0.6)	DCE	85	92	100
9	0.4	TBHP(0.4)	DCE	85	91	100
10	0.4	TBHP(0.6)	DCE	85	84	100
11	0.4	TBHP(0.8)	DCE	85	86	100
12	0.4	TBHP(0.4)	Ethanol	85	29	100
13	0.4	TBHP(0.4)	Methanol	85	40	100
14	0.4	TBHP(0.4)	Acetonitrile	85	19	100
15	0.4	TBHP(0.4)	Chloroform	85	82	100
16	0.4	TBHP(0.4)	n-Hexane	85	53	100
17	0.4	TBHP(0.4)	DCE	70	48	100
18	0.4	TBHP(0.4)	DCE	60	32	100
19	0.4	TBHP(0.4)	DCE	r.t.	24	100

^aReaction conditions for [Co (tp)₂(H₂O)₂].C₂H₅OH (1): cis-cyclooctene (0.2 mmol), solvent (1 ml) and 5 hr.

^bGC conversions based on starting alkenes.

^cSelectivity to epoxide = ((epoxide) / (epoxide + other products)) × 100.

TABLE 5 Catalytic oxidation of various alkenes with TBHP in water by (1) or (2)^a

Entry	Catalyst	Substrate	Time (hr)	Conversion (%) ^b	Selectivity (%) ^c
1	1	Cis cyclooctene	5	91	100
2	1	Styrene	5	94	54
3	1	4-methyl styrene	5	95	53
4	1	4-methoxy styrene	5	76	80
5	1	α -methyl styrene	5	91	>99
6	1	Cis stilbene	5	56	47
7	1	Trans stilbene	5	61	55
8	1	1-octene	5	39	38
9	1	Trans -2-octene	5	68	61
10	2	Cis cyclooctene	1	94	100
11	2	Styrene	1	98	60
12	2	4-methyl styrene	1	96	58
13	2	4-methoxy styrene	1	79	80
14	2	α -methyl styrene	1	91	>99
15	2	Cis stilbene	1	62	59
16	2	Trans stilbene	1	69	64
17	2	1-octene	1	49	42
18	2	Trans -2-octene	1	71	68

^aReaction conditions: substrate (0.2 mmol), TBHP in water (0.4 mmol), catalyst (0.4 mol%), C₂H₄Cl₂ (1 ml) and 85 °C.

^bGC conversions based on starting alkenes.

^cSelectivity to epoxide = ((epoxide) / (epoxide + other products)) \times 100.

catalysts according to the oxidation protocol mentioned above; the catalytic results are shown in Table 5. Good catalytic activity and good selectivity were found for different substrates. Excellent yield and high selectivity were observed for cis-cyclooctene for both catalysts (Table 5, entry 1 and 10). The lowest conversions were observed for terminal alkenes such as 1-octene (Table 5, entry 8 and 17), because the percentage of conversion and selectivity for epoxidation of the terminal alkenes is reduced by the fraction of internal alkenes. The results of the epoxidation reaction in presence of (2) are also compiled in (Table 5, entry 10–18). Again, we observe that the reaction-time is reduced and the percentage of the conversion to epoxide is increased. While most reported methods require high loadings of a molybdenum catalyst and difficult conditions, we happily report that both our cobalt complex (1) and our Co₃O₄ n.p.s activate the epoxidation reaction.^[63–66]

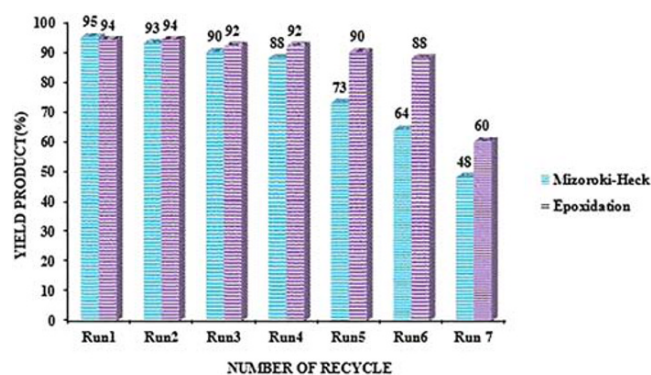


FIGURE 8 Recyclability and reusability study of the Co₃O₄ n.p.s (catalyst 2) in the MH and AE reactions

3.6 | Recoverability

The reusability of the catalyst (2) is, of course, a primordial concern. In order to assess this reusability for the

nanocrystals (**2**), we chose the following procedure: after each cycle the nanocrystals were separated from the reaction mixture by filtration, twice washed with distilled water and PEG (since **2** is insoluble in PEG), dried at 55 °C for 1 hr and then reused for another MH reaction of iodobenzene, methyl acrylate, and K_3PO_4 at 130 °C for 2 hr (Figure 8). After six cycles the reaction yield was reduced to 48% and this decrease in the catalytic activity is mainly attributed to structural changes of the catalyst **2**. The reusability of catalyst **2** in the AE reaction in DCE is shown in Figure 8. After six uses the reaction yield was reduced to 60%, which suggests that this is also an

appropriate catalyst for the AE reaction. This decrease in the catalytic activity is mainly attributed to structural changes of the n.p.s **2**; this change in the structure is confirmed by comparing the IR spectra of a fresh and a catalyst recycled (Figure S6) in the AE reaction. As it is clear from Figures 8 and S6, the results suggest that the catalyst **2** has a mild recyclability owing to structural changes and the decomposition of the n.p.s.

We note that **2**, compared with earlier methods, is catalytically efficient in mild media (low amount of solvent, moderate temperature and safe metal), in both the MH cross coupling and the AE reactions, presenting

FIGURE 9 Recyclability and reusability study of the $[Co(tp)_2(H_2O)_2] \cdot C_2H_5OH$ (catalyst 1) in the MH and AE reactions

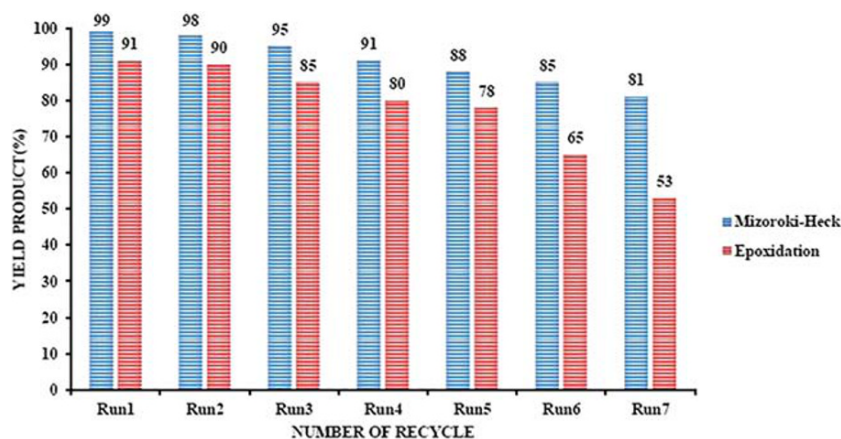


TABLE 6 Comparison of catalytic activities of our catalysts with literature examples for the MH reaction between iodobenzene and methyl acrylate and the AE reaction of cyclooctene

Entry	Reaction	Catalyst ^{ref}	Reaction conditions	Time (hr)	Yield (%)
1	Mizoroki-Heck	Co@MicroCS ^[14]	Co (3 mol% (21 μmol)) in DMAc at 140 °C	8	82
2		Co-MS@MNPs/CS ^[13]	Co (1.1 mol %) in PEG at 80 °C	1	88
3		Nano Co ^[67]	Co (2 mol%) in NMP at 130 °C	14	78
4		Co/Al ₂ O ₃ ^[68]	Co (10 mol%) in NMP at 150 °C	24	56
5		Co-B ^[62]	Co (5 mol %) in water/DMF (5/5) at 130 °C	12	98
6		Present catalyst $[Co(tp)_2(H_2O)_2] \cdot C_2H_5OH$ (1)	Co complex (0.4 mol %) in PEG at 130 °C	2	99
7		Present catalyst Co ₃ O ₄ (2)	Catalyst (0.4 mol %) in PEG at 130 °C	2	95
8	Epoxidation of alkenes	MOF $[Co_3(BDC)_3(DMF)_2(H_2O)_2]_n$ ^[69]	Catalyst (0.01 mmol) in CH ₃ CN at 75 °C	7	67
9		Co ₃ O ₄ ^[38]	Co (0.01 mmol) in CH ₂ Cl ₂ :CH ₃ OH at 70 °C	1	85
10		MOF $[NiCo(\mu_2-tp)(\mu_4-tp)(4,40-bpy)_2]_n$ ^[1]	Catalyst (100 mg) in CHCl ₃	2	38
10		NiO/Co ₃ O ₄ nanocatalyst ^[70]	Catalyst (100 mg) in CHCl ₃	4	76
11		Present catalyst $[Co(tp)_2(H_2O)_2] \cdot C_2H_5OH$ (1)	Co complex (0.4 mol %) in DCE at 85 °C	5	91
12		Present catalyst Co ₃ O ₄ (2)	Catalyst (0.4 mol %) in DCE at 85 °C	1	94

significantly lower reaction-times, excellent percentage of conversion and selectivity.

In the following, the reusability of the catalyst (**1**) is, of course, a primordial concern. In order to assess this for the complex (**1**) we chose the following procedure: After each cycle these complex were separated from the reaction mixture by filtration and then twice washed with distilled water (since (**1**) is insoluble in water), dried at 65 °C for 1 hr, and then reused for another MH reaction of iodobenzene, methyl acrylate, and K₃PO₄ at 130 °C for 2 hr (Figure 9). After six cycles the reaction yield was reduced to 81% and this decrease in the catalytic activity is mainly attributed to structural changes of the catalyst **1**. The reusability of catalyst (**1**) in the AE reaction in DCE is shown in Figure 9. After six uses the reaction yield was reduced to 53%, which suggests that this is also an appropriate catalyst for the MH reaction. This decrease in the catalytic activity is mainly attributed to structural changes of the complex **1**, this change in the structure is confirmed by comparison of IR data from the fresh and the recycled catalyst (Figure S7) in the MH reaction. As it is clear from Figures 9 and S7, the results suggest that the catalyst **1** has mild recyclability owing to structural changes and the decomposition of the complex.

A comparison of the catalytic reactivity of our catalysts **1** and **2** with recently reported catalytic systems in the MH and AE reactions is summarised in Table 6. Both our catalysts activate, under mild conditions, in both reactions and yield short reaction-times, but their most salient benefits are the low cost of the metal in comparison with palladium, their functioning in low amounts of solvent and the low amount of catalyst.

4 | CONCLUSIONS

The carboxamide N-(thiazole-2-yl) picolinamide (**Htp**) has been prepared in the green TBAB and incorporated into [Co^{II}(tp)₂(H₂O)₂] C₂H₅OH. This ethanolate was then stripped of **tp** and its water by thermal decomposition at 600 °C for 2 hr to yield spinel Co₃O₄ nanoparticles of an average diameter of 32 nm and appropriate dispersion. The coordination geometry around Co^{II} is distorted octahedral in the complex and cubic in the nps. We have characterised the catalyst from various aspects by: FTIR, CHNS, UV-Vis, NMR, TGA, DSC, XRD, FE-SEM and CV. Mild and sustainable reaction conditions (PEG as solvent, 130 °C, 2 hr), applied to a good two dozens of olefins, showed the ethanolate as well as the Co₃O₄ nps to be powerful catalysts in the MH cross coupling reaction, affording good yields with low metal contamination in a simple way. Co (II) complexes and Co₃O₄ nps are also activated

in the AE reaction. This straightforward and sustainable chemistry without expensive metals provides useful and eco-efficient catalysts bearing many useful properties: their green and easy way of synthesis (without using toxic agents and solvents) and good efficiency in the MH coupling and AE reactions.

ACKNOWLEDGMENTS

We gratefully acknowledge the funding support received for this project from the Sharif University of Technology (SUT).

ORCID

Mahsa Kiani  <https://orcid.org/0000-0003-3341-5272>

Mojtaba Bagherzadeh  <https://orcid.org/0000-0003-3009-3693>

Farzaneh Fadaei-Tirani  <https://orcid.org/0000-0002-7515-7593>

REFERENCES

- [1] J. Magano, J. R. Dunetz, *Chem. Rev.* **2011**, *111*, 2177.
- [2] C. Torborg, M. Beller, *Adv. Synth. Catal.* **2009**, *351*, 3027.
- [3] I. P. Beletskaya, A. V. Cheprakov, *Chem. Rev.* **2000**, *100*, 3009.
- [4] M. B. Rodrigues, R. A. Halfen, S. C. Feitosa, C. P. Frizzo, M. A. Martins, N. Zanatta, A. A. Merlo, H. G. Bonaccorso, *J. Mol. Liq.* **2019**, *287*, 110896.
- [5] S. Sabounchei, M. Ahmadianpoor, A. Yousefi, A. Hashemi, M. Bayat, A. Sedghi, F. A. Bagherjeri, R. Gable, *RSC Adv.* **2016**, *6*, 28308.
- [6] H. Mahmoudi, F. Valentini, F. Ferlin, L. A. Bivona, I. Anastasiou, L. Fusaro, C. Aprile, A. Marrocchi, L. Vaccaro, *Green Chem.* **2019**, *21*, 355.
- [7] M. E. Martínez-Klimov, P. Hernández-Hipólito, M. Martínez-García, T. E. Klimova, *Catal. Today* **2018**, *305*, 58.
- [8] D. Roy, Y. Uozumi, *Adv. Synth. Catal.* **2018**, *360*, 602.
- [9] Y. Guo, J. Li, X. Shi, Y. Liu, K. Xie, Y. Liu, Y. Jiang, B. Yang, R. Yang, *Appl. Organomet. Chem.* **2017**, *31*, e3592.
- [10] C. Liu, M. Szostak, *Angewandte Chemie* **2017**, *129*, 12892.
- [11] S.-S. Wang, G.-Y. Yang, *Catal. Sci. Technol.* **2016**, *6*, 2862.
- [12] Y. Lei, G. Lan, D. Zhu, R. Wang, X. Y. Zhou, G. Li, *Appl. Organomet. Chem.* **2018**, *32*, e4421.
- [13] A. R. Hajipour, F. Rezaei, Z. Khorsandi, *Green Chem.* **2017**, *19*, 1353.
- [14] Y. Bao, L. Shao, G. Xing, C. Qi, *Int. J. Biol. Macromol.* **2019**, *130*, 203.
- [15] P. Wang, G. Zhang, H. Jiao, X. Deng, Y. Chen, X. Zheng, *Appl. Catal. Gen.* **2015**, *489*, 188.
- [16] F. Diler, H. Burhan, H. Genc, E. Kuyuldar, M. Zengin, K. Cellat, F. Sen, *J. Mol. Liq.* **2019**, 111967.
- [17] B. S. Lane, K. Burgess, *Chem. Rev.* **2003**, *103*, 2457.
- [18] A. K. Yudin, *Aziridines and epoxides in organic synthesis*, Weinheim City, Germany: John Wiley & Sons; **2006**.
- [19] A. Blanckenberg, R. Malgas-Enus, *Catal. Rev.* **2019**, *61*, 27.
- [20] A. Z. Halimehjani, L. Hasani, M. A. Alaei, M. R. Saidi, *Tetrahedron Lett.* **2016**, *57*, 883.
- [21] D. E. Lynch, R. Hayer, S. Beddows, J. Howdle, C. D. Thake, *J. Heterocyclic Chem.* **2006**, *43*, 191.

- [22] D. Bansal, G. Hundal, R. Gupta, *Eur. J. Inorg. Chem.* **2015**, 2015, 1022.
- [23] R. Del Litto, V. Benessere, F. Ruffo, C. Moberg, *Eur. J. Organ. Chem.* **2009**, 2009, 1352.
- [24] L. Yang, R.-N. Wei, R. Li, X.-G. Zhou, J.-L. Zuo, *J. Mol. Catal. A: Chem.* **2007**, 266, 284.
- [25] R. M. Lanigan, T. D. Sheppard, *Eur. J. Organ. Chem.* **2013**, 2013, 7453.
- [26] D. Bansal, S. Pandey, G. Hundal, R. Gupta, *New J. Chem.* **2015**, 39, 9772.
- [27] D. Bansal, R. Gupta, *Dalton Trans.* **2017**, 46, 4617.
- [28] E. Valeur, M. Bradley, *Chem. Soc. Rev.* **2009**, 38, 606.
- [29] D. Bansal, G. Kumar, G. Hundal, R. Gupta, *Dalton Trans.* **2014**, 43, 14865.
- [30] A. K. Singh, R. Mukherjee, *Inorg. Chem.* **2005**, 44, 5813.
- [31] L. Shen, C. Wang, *Electrochim. Acta* **2014**, 133, 16.
- [32] Y. Huang, C. Chen, C. An, C. Xu, Y. Xu, Y. Wang, L. Jiao, H. Yuan, *Electrochim. Acta* **2014**, 145, 34.
- [33] D. V. Dreifus. Propriedades microestruturais e magnéticas de policristais de V_2O_5 , CoV_2O_6 e Co_3O_4 sintetizadas por método Pechini, **2014**.
- [34] S. R. Gawali, A. C. Gandhi, S. S. Gaikwad, J. Pant, T.-S. Chan, C.-L. Cheng, Y.-R. Ma, S. Y. Wu, *Sci. Rep.* **2018**, 8, 249.
- [35] C. Kaçar, B. Dalkiran, P. E. Erden, E. Kiliç, *Appl. Surf. Sci.* **2014**, 311, 139.
- [36] S. Meghdadi, M. Amirnasr, Z. Azarkamanzad, K. Schenk Joß, F. Fadaee, A. Amiri, S. Abbasi, *J. Coord. Chem.* **2013**, 66, 4330.
- [37] S. Meghdadi, M. Amirnasr, M. Kiani, F. Fadaei Tirani, M. Bagheri, K. J. Schenk, *J. Coord. Chem.* **2017**, 70, 2409.
- [38] A. Askarinejad, M. Bagherzadeh, A. Morsali, *Appl. Surf. Sci.* **2010**, 256, 6678.
- [39] Y. Ikeda, T. Nakamura, H. Yorimitsu, K. Oshima, *J. Am. Chem. Soc.* **2002**, 124, 6514.
- [40] R. A. Budnik, J. K. Kochi, *J. Org. Chem.* **1976**, 41, 1384.
- [41] X-AREA; Version 1.36, Stoe & Cie, Darmstadt, Germany. **2006**.
- [42] X-RED32; Version 1.31, Stoe & Cie GmbH, Darmstadt, Germany. **2005**.
- [43] G. M. Sheldrick, *Acta Crystallogr. Section a: Found. Crystallogr.* **2008**, 64, 112.
- [44] G. M. Sheldrick, *Acta Crystallogr. Section C: Struct. Chem.* **2015**, 71, 3.
- [45] A. L. Spek, *Acta Crystallogr. Section C: Struct. Chem.* **2015**, 71, 9.
- [46] M. Amirnasr, R. S. Erami, S. Meghdadi, *Sens. Actuators B* **2016**, 233, 355.
- [47] M. M. Khodaei, A. R. Khosropour, K. Ghozati, *Tetrahedron Lett.* **2004**, 45, 3525.
- [48] K. M. Docherty, C. F. Kulpa Jr., *Green Chem.* **2005**, 7, 185.
- [49] S. Meghdadi, M. Amirnasr, S. H. M. Sadat, K. Mereiter, A. Amiri, *Monatshfte für Chemie-Chem. Monthly* **2014**, 145, 1583.
- [50] S. C. Chang, J. K. Ma, J. T. Wang, N. C. Li, *J. Coord. Chem.* **1972**, 2, 31.
- [51] S. Meghdadi, M. Amirnasr, A. Amiri, Z. M. Mobarakeh, Z. Azarkamanzad, *C. R. Chim.* **2014**, 17, 477.
- [52] S. H. Sumrra, M. Hanif, Z. H. Chohan, M. S. Akram, J. Akhtar, S. M. Al-Shehri, *J. Enzyme Inhib. Med. Chem.* **2016**, 31, 590.
- [53] L. Forlani, P. De Maria, E. Foresti, G. Pradella, *J. Org. Chem.* **1981**, 46, 3178.
- [54] S. Meghdadi, M. Amirnasr, M. Zhiani, F. Jallili, M. Jari, M. Kiani, *Electrocatalysis* **2017**, 8, 122.
- [55] S. Asadzadeh, M. Amirnasr, S. Meghdadi, F. F. Tirani, K. Schenk, *Int. J. Hydrogen Energy* **2018**, 43, 4922.
- [56] S. Meghdadi, M. Amirnasr, M. H. Habibi, A. Amiri, V. Ghodsi, A. Rohani, R. W. Harrington, W. Clegg, *Polyhedron* **2008**, 27, 2771.
- [57] M. Kazemnejadi, Z. Rezazadeh, M. A. Nasser, A. Allahresani, M. Esmaeilpour, *Green Chem.* **2019**, 21, 1718.
- [58] A. V. Piskunov, K. I. Pashanova, A. S. Bogomyakov, I. V. Smolyaninov, A. G. Starikov, G. K. Fukin, *Dalton Trans.* **2018**, 47, 15049.
- [59] M. Bagherzadeh, F. Ashouri, L. Hashemi, A. Morsali, *Inorg. Chem. Commun.* **2014**, 44, 10.
- [60] M. Bagherzadeh, H. Mahmoudi, S. Ataie, M. Bahjati, R. Kia, P. R. Raithby, L. Vaccaro, *Mol. Catal.* **2019**, 474, 110406.
- [61] A. R. Hajipour, Z. Khorsandi, M. Mortazavi, H. Farrokhpour, *RSC Adv.* **2015**, 5, 107822.
- [62] Z. Zhu, J. Ma, L. Xu, L. Xu, H. Li, H. Li, *ACS Catal.* **2012**, 2, 2119.
- [63] M. Bagherzadeh, S. Ataie, H. Mahmoudi, J. Janczak, *Inorg. Chem. Commun.* **2017**, 84, 63.
- [64] J. Liu, T. Chen, P. Jian, L. Wang, *Chin. J. Catal.* **2018**, 39, 1942.
- [65] B. Li, X. Luo, Y. Zhu, X. Wang, *Appl. Surf. Sci.* **2015**, 359, 609.
- [66] Z. Li, S. Wu, C. Yang, Y. Ma, X. Fu, L. Peng, J. Guan, Q. Kan, *Mol. Catal.* **2017**, 432, 267.
- [67] H. Qi, W. Zhang, X. Wang, H. Li, J. Chen, K. Peng, M. Shao, *Cat. Com.* **2009**, 10, 1178.
- [68] S. Iyer, V. V. Thakur, *J. Mol. Catal. A: Chem.* **2000**, 157, 275.
- [69] F. Ashouri, M. Zare, M. Bagherzadeh, *Inorg. Chem. Commun.* **2015**, 61, 73.
- [70] A. Abbasi, M. Soleimani, M. Najafi, S. Geranmayeh, *J. Mol. Struct.* **2017**, 1133, 458.

SUPPORTING INFORMATION

Additional supporting information may be found online in the Supporting Information section at the end of this article.

How to cite this article: Kiani M, Bagherzadeh M, Meghdadi S, Fadaei-Tirani F, Babaie M, Schenk-Joß K. Promising new catalytic properties of a Co (II)-carboxamide complex and its derived Co_3O_4 nanoparticles for the Mizoroki-Heck and the Epoxidation reactions. *Appl Organomet Chem.* 2020;e5911. <https://doi.org/10.1002/aoc.5911>

APPENDIX A: Supplementary Data

The supplementary information consists of full characterisations of the ligand and the complex and the ^1H and ^{13}C NMR spectra of the products. Crystallographic data for

the structural analyses have been deposited with the Cambridge Crystallographic Data Centre, CCDC No **1885351**. These data can be obtained free of charge from The Cambridge Crystallographic Data Centre *via* www.ccdc.cam.ac.uk/data_request/cif.